Vibrational Properties of $Cu(Pz)_2(ClO_4)_2$: Evidence for Enhanced Low-Temperature Hydrogen Bonding in Square $S = {}^1/_2$ Molecular Antiferromagnets

J. Choi, J. D. Woodward, and J. L. Musfeldt*

Department of Chemistry, University of Tennessee, Knoxville, Tennessee 37996

C. P. Landee

Department of Physics, Clark University, Worcester, Massachusetts 01610

M. M. Turnbull

Carlson School of Chemistry and Biochemistry, Clark University, Worcester, Massachusetts 01610

Received March 4, 2003. Revised Manuscript Received April 22, 2003

We report the variable temperature vibrational properties of the two-dimensional $S = {}^1/_2$ quantum Heisenberg antiferromagnet $Cu(Pz)_2(ClO_4)_2$. With decreasing temperature, softening is observed in the $\nu_4(ClO_4)$ mode. In addition, the resonance frequencies of several pyrazine ring-related modes are temperature independent. This unusual behavior is attributed to enhanced hydrogen bonding interactions between the ClO_4^- counterion and the pyrazine rings in a neighboring layer, in line with the recently observed low-temperature red-shifts of numerous vibrational modes in the one-dimensional analogue, copper pyrazine dinitrate ($Cu(Pz)(NO_3)_2$). The proposed change in hydrogen bonding and the low-temperature symmetry breaking, made manifest by the concomitant doublet structure of several pyrazine-related modes, is supported by an analysis of the structure.

I. Introduction

Chemical structure/physical property relationships in molecular copper complexes continue to attract the sustained attention of the materials chemistry community. The structures of these low-dimensional materials range from linear chains to two-dimensional (2D) layers. Examples of such compounds include one-dimensional (1D) chains such as copper pyrazine dinitrate ($Cu(Pz)(NO_3)_2$), $(X)_2CuBr_4$ ladders, and 2D sheets such as $Cu(Pz)_2X_2$ (where X is a counterion).[1−5] From the magnetic perspective, the transition between 1 and 2D order in these $S = {}^1/_2$ quantum Heisenberg antiferromagnets can be viewed as the change in the ratio of exchange constants, J'/J (where, J' and J are the interchain and intrachain exchange constant, respectively), going from 0 (a pure chain) to 1 (a square lattice). These chemically related materials are thus physical manifestations of ideal quantum antiferromagnets, the systematic investigation of which is of considerable theoretical interest.[6−10]

The 300 K crystal structure of $Cu(Pz)_2(ClO_4)_2$ is shown in Figure 1. Each layer consists of rectangular arrays of copper atoms bridged by pyrazine ligands. In addition, two disordered ClO_4^- tetrahedra are semicoordinated, one on top and the other on the bottom, to each Cu^{2+}, with $C2/m$ symmetry.[11,12] As with many other low-dimensional molecular copper systems, the structure of $Cu(Pz)_2X_2$ compounds is influenced by the counterions. With monovalent, poorly coordinating anions (e.g., ClO_4^-, BF_4^-, and PF_6^-), 2D structures are formed.[5,13] Various magnetic parameters, such as the exchange constant and the critical field for saturation of the magnetization, are closely connected with certain architectural nuances such as bond lengths, ring tilt, and counterion identity. For example, in $Cu(Pz)_2(ClO_4)_2$, the coordinated ClO_4^- anions are disordered and crystallographically inequivalent. The closest distance between coordinated oxygen and copper is within the repulsive range. Therefore, in order to minimize nonbonding interactions between ClO_4^- ions, the

* To whom correspondence should be addressed.

(1) Villa, J. F.; Hatfield, W. E. *J. Am. Chem. Soc.* **1971**, *93*, 4081.
(2) Hammar, P. R.; Stone, M. B.; Reich, D. H.; Broholm, C.; Gibson, P. J.; Turnbull, M. M.; Landee, C. P.; Oshikawa, M. *Phys. Rev. B* **1999**, *59*, 1008.
(3) Mennenga, G.; de Jongh, L. J.; Huiskamp, W. J.; Reedick, J. *J. Magn. Magn. Mater.* **1984**, *44*, 89.
(4) Landee, C. P.; Turnbull, M. M.; Galeriu, C.; Giantsidis, J.; Woodward, F. M. *Phys. Rev. B* **2001**, *63*, 100402.
(5) Turnbull, M. M.; Albrecht, A. S.; Jameson, G. B.; Landee, C. P. *Mol. Cryst. Liq. Cryst.* **1999**, *334*, 957.
(6) Manousakis, E. *Rev. Mod. Phys.* **1991**, 63, 1.
(7) Yang, M. S.; Mütter, K. H. *Z. Phys. B: Condens. Matter* **1997**, *104*, 117.
(8) Zhitomirsky, M. E.; Nikuni, T. *Phys. Rev. B* **1998**, *57*, 5013.
(9) Zhitomirsky, M. E.; Chernyshev, A. L. *Phys. Rev. Lett.* **1999**, *82*, 4536.
(10) Fledderjohann, A.; Mütter, K.-H.; Yang, M.-S.; Karbach, M. *Phys. Rev. B* **1998**, *57*, 956.
(11) Darriet, J.; Haddad, M. S.; Duesler, E. N.; Hendrickson, D. N. *Inorg. Chem.* **1979**, *18*, 2679.
(12) Haddad, M. S.; Hendrickson, D. N.; Cannady, J. P.; Drago, R. S.; Bieksza, D. S. *J. Am. Chem. Soc.* **1979**, *101*, 898.
(13) Woodward, F. M.; Landee, C. P.; Turnbull, M. M. Unpublished data.

10.1021/cm030049e CCC: $25.00
Published on Web 06/07/2003

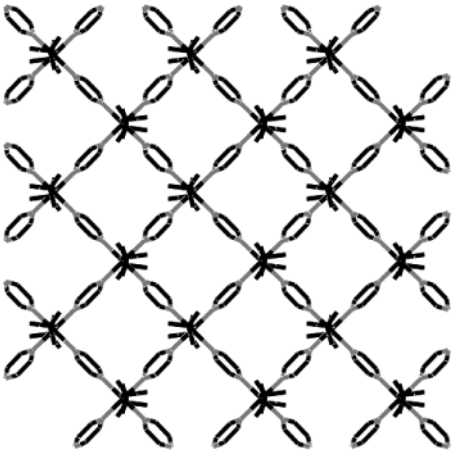

Figure 1. Single layer view of $Cu(Pz)_2(ClO_4)_2$.

Cu−O−Cl angle is larger than that in other similar compounds such as $Cu(NH_2CH_2CH_2SCH_3)_2(ClO_4)_2$.[14] At low temperatures, the crystal symmetry is reduced to *C*2/*c*.[13] This phase is characterized by ordered ClO_4^- ions and two sets of identical pyrazine pairs, with tilt angles of 62.8° and 69.1° with respect to the Cu−N coordination plane.[13]

As in all of these low-dimensional copper complexes, the dihedral angle between the pyrazine-ring plane and the Cu−N coordination plane has a strong influence on the magnitude of superexchange interactions. This is because superexchange takes place through the pyrazine rings.[2] At low temperatures, the superexchange interaction results in a herringbone magnetic configuration for $Cu(Pz)_2(ClO_4)_2$ rather than a square lattice assignment due to the difference in pyrazine-ring tilt angle.[13] However, susceptibility measurements show that $Cu(Pz)_2(ClO_4)_2$ fits the 2D quantum Heisenberg antiferromagnet model very well, with an exchange constant $J = -17.8$ K and $g = 2.11$.[15,5] The critical field for saturation of the magnetization is estimated to be 52.5 T. This value is large compared to the 14.6 T saturation field of the 1D analogue $Cu(Pz)(NO_3)_2$,[5,2] but it is small compared with that of $TlCuCl_3$ (150 T), $SrCu_2O_3$ (300 T), and $CuGeO_3$ (500 T).[16−18] Indeed, the major attraction of these 2D molecular copper complexes is that their critical fields are both tunable and experimentally accessible with powered steady and pulsed magnet systems.

The recent discovery of interchain hydrogen bonding in the 1D analogue, $Cu(Pz)(NO_3)_2$, was both unexpected and dramatic.[19] The change in electrostatic interaction was evidenced by the softening of numerous vibrational modes with decreasing temperature due to an increase in the corresponding bond lengths. The same effect is observed in chemically substituted $Cu(Pz)(NO_3)_2$-based chain compounds as well, although the degree of softening is less than that in the unsubstituted material.[19] In this work, we extend our investigation of long-range electrostatic interactions in molecular copper complounds to the 2D $S = {}^1/_2$ quantum Heisenberg antiferromagnet $Cu(Pz)_2(ClO_4)_2$. Although the mode softening in this compound is much less than that in $Cu(Pz)(NO_3)_2$, the slight red-shift of a perchlorate-related mode with decreasing temperature as well as the temperature independence of several pyrazine ring-related modes suggests the enhancement of low-temperature hydrogen bonding interactions in $Cu(Pz)_2(ClO_4)_2$. Doublet structures in several pyrazine-related modes also point to a subtle symmetry breaking at low temperature, which can be connected with the character of the hydrogen bonding. We suggest that hydrogen bonding interactions may influence the structure and magnetism of this entire family of low-dimensional quantum antiferromagnets.

II. Experimental Section

$Cu(Pz)_2(ClO_4)_2$ crystals were grown from aqueous solutions containing a 1:2 molar ratio of $Cu(ClO_4)_2$ and pyrazine. The resultant samples are thin, square-shaped plates with typical dimensions $\sim 2 \times 2 \times 0.5$ mm^3. $Cu(Pz)_2(ClO_4)_2$ was combined with two different matrix materials, paraffin and KCl, to prepare pellets for far- and middle-infrared transmittance measurements, respectively. We performed variable temperature transmittance experiments using both Bruker 113V and Equinox 55 Fourier transform infrared spectrometers, the latter equipped with an IR Scope II infrared microscope, covering the 30−5000 cm^{-1} spectral range. The resolution was 0.5 cm^{-1}. It is our experience that both low temperature and high spectral resolution are helpful to resolve weak modes and narrow line shapes. For peak fitting purposes, absorbance was calculated from transmittance as $-\ln T(\omega)$, where T is the transmittance. Peak positions and integrated oscillator strengths were determined by standard peak fit procedures.

Room-temperature X-ray diffraction data were collected at 293(2) K using a Bruker/Siemens SMART APEX instrument (Mo Kα radiation, $\lambda = 0.71073$ Å). Cell parameters were retrieved using SMART[20] software and refined using SAINTPlus[21] on all observed reflections. Data reduction and correction for Lp and decay were performed using the SAINTPlus software. Absorption corrections were applied using SADABS.[22] The structure was solved by direct methods and refined by least-squares method on F^2 using the SHELXTL program package.[23] Low-temperature data were collected at 163(2) K using a CCD area detector (Mo Kα radiation, $\lambda = 0.71073$ Å). Data collection, cell refinement, and data reduction were performed using Bruker SMART and SAINT.[24] Solution and refinement were as described.

III. Results and Discussion

Figure 2 displays the 10 K infrared transmittance of $Cu(Pz)_2(ClO_4)_2$. Among the many sharp features in the far-infrared spectrum (upper panel), the clusters at $\sim$120, 280, and 500 cm^{-1} are particularly notable. These features are due to Cu−O and Cu−N stretching, and

(14) Haddad, M. S.; Duesler, E. N.; Hendrickson, D. N. *Inorg. Chem.* **1979**, *18*, 141.
(15) Albrechet, A. S.; Landee, C. P.; Slanic, Z.; Turnbull, M. M. *Mol. Cryst. Liq. Cryst.* **1997**, *305*, 333.
(16) Shiramura, W.; Takatsu, K.; Tanaka, H.; Kamishima, K.; Takahashi, M.; Mitamura, H.; Goto, T., *J. Phys. Soc. Jpn.* **1997**, *66*, 1900.
(17) Azuma, M.; Hiroi, Z.; Takano, M.; Ishida, K.; Kitaoka, Y., *Phys. Rev. Lett.* **1994**, *73*, 3463.
(18) Nijiri, H.; Shimamoto, Y.; Miura, N.; Hase, M.; Uchinokura, K.; Kojima, J.; Tanaka, I.; Shilbuya, Y. *Phys. Rev. B.* **1995**, *52*, 12749.
(19) Jones, B. R.; Varughese, P. A.; Olejniczak, I.; Pigos, J. M.; Musfeldt, J. L.; Landee, C. P.; Turnbull, M. M.; Carr, G. L. *Chem. Mater.* **2001**, *13*, 2127.
(20) *SMART*: *v.5.625, Bruker Molecular Analysis Research Tool*; Bruker AXS: Madison, WI, 2001.
(21) *SAINTPlus: v. 6.22, Data Reduction and Correction Program*; Bruker AXS: Madison, WI, 2001.
(22) Sheldrick, G. M. *SADABS: v.2.01, an empirical absorption correction program*; Bruker AXS Inc.: Madison, WI, 2001.
(23) Sheldrick, G. M. *SHELXTL: v. 6.10, Structure Determination Software Suite*; Bruker AXS Inc.: Madison, WI, 2001.
(24) *SMART and SAINT. Area Detector Control and Integration Software*; Bruker AXS, Inc.: Madison, WI, 1996.

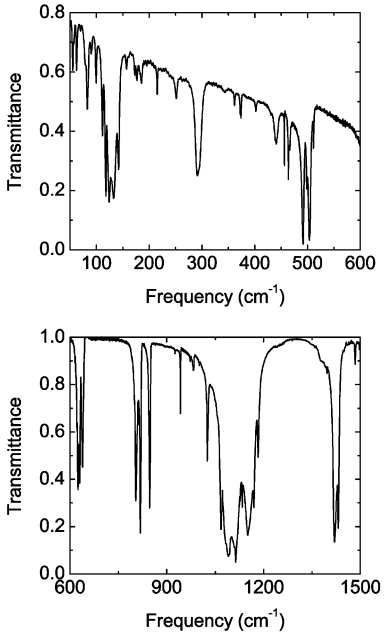

Figure 2. Far (upper panel) and middle (lower panel) infrared transmittance spectrum of $Cu(Pz)_2(ClO_4)_2$ at 10 K.

pyrazine ring out-of-plane deformation, respectively.[25] At 300 K, the 120 cm^{-1} feature has a broad, asymmetric shape, indicating the superposition of several modes. With decreasing temperature, line widths are reduced, allowing the underlying multiplet structure to be clearly distinguished. We do not resolve any fine structure in the 280 cm^{-1} Cu−N stretching mode at 10 K, indicating that the C−N distances in this molecular lattice are nearly identical. The pyrazine ring-related mode near 500 cm^{-1} has a doublet structure at 300 K. With decreasing temperature, two smaller features gradually develop ∼7 cm^{-1} above each of the main features. The appearance of this fine structure suggests a subtle change in the nature of the pyrazine position. All vibrational modes harden with decreasing temperature in the far-infrared region.

The lower panel of Figure 2 displays the 10 K middle-infrared transmittance spectrum of $Cu(Pz)_2(ClO_4)_2$. The group of features near 630 cm^{-1} is assigned as $\nu_4(ClO_4)$.[26,27] Some components of this mode display an unusual low-temperature softening, which will be discussed in detail later. The set of peaks near 820 cm^{-1} is attributed to pyrazine ring C−H out-of-plane deformation.[28] Low temperature doublets are visible on several features between 800 and 860 cm^{-1} (upper right panel in Figure 3). In the region from 1000 to 1200 cm^{-1}, the spectrum is very rich, with a large number of vibrational modes superimposed upon each other. Due to the complexity of the line shape, it is difficult to make a definitive assignment for each peak. However, on the basis of the mode assignments of other pyrazine- and perchlorate-based compounds, this feature is certainly related to the superposition of pyrazine ring and perchlorate motions,[26−28] specifically, a combination of $\nu_3(ClO_4)$ and overlaid modes of pyrazine ring stretching,

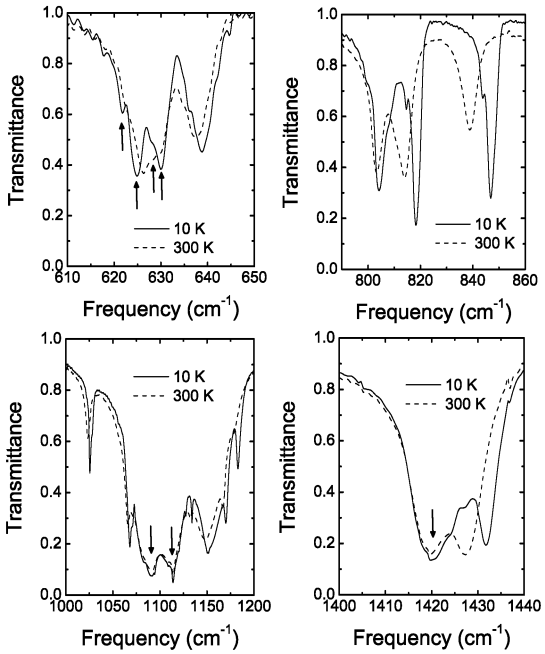

Figure 3. Transmittance of $Cu(Pz)_2(ClO_4)_2$ at 10 K (—) and 300 K (- - -) in different frequency regions. The features indicated with arrows display softening or no change in frequency with decreasing temperature.

Table 1. Assignment of Vibrational Modes in $Cu(Pz)_2(ClO_4)_2$

peak position at 300 K	motion
120 cm^{-1} cluster	Cu−O stretching
280 cm^{-1}	Cu−N stretching
500 cm^{-1} group	Pz ring out-of-plane deformation
620 cm^{-1} group	$\nu_4(ClO_4)$
820 cm^{-1} group	Pz ring C−H out-of-plane deformation
940−990 cm^{-1} group	Pz ring stretching + ring in-plane bending
1000−1200 cm^{-1} cluster	$\nu_3(ClO_4)$ + Pz ring stretching + ring in-plane bending + C−H in-plane bending
1420 cm^{-1} group	Pz ring stretching + C−H in-plane bending

ring in-plane bending, plus C−H in-plane bending. A summary of our peak assignments is given in Table 1. The majority of the aforementioned vibrational modes shift to higher frequencies at low temperature. There is nothing surprising in this trend; most modes harden at low temperature due to well-known lattice contraction effects.[19] However, a select number of vibrational features in $Cu(Pz)_2(ClO_4)_2$ show a different behavior. Using our understanding of the microscopic nature of the motion, the observed trends can be connected with enhanced low-temperature hydrogen bonding interactions and a subtle low-temperature structural distortion in this compound.

Close-up views of several selected vibrational modes of $Cu(Pz)_2(ClO_4)_2$ are shown in Figure 3. Here, the behavior of the multiplet near 620 cm^{-1} is particularly revealing. The two modes near 622 and 625 cm^{-1} display low-temperature softening, and two other modes near 628 and 630 cm^{-1} are insensitive to temperature over the range of our measurements. The softening of the 622 and 625 cm^{-1} modes takes place gradually, with nonlinear temperature dependence, and saturates near 50 K. We can quantify these effects by plotting the center frequency of each mode as a function of temper-

(25) Child, M. D.; Percy, G. C. *Spectrosc. Lett.* **1977**, *10*, 71.
(26) Nakamoto, K. *Infrared Spectra of Inorganic and Coordination Compounds*, 3rd ed.; John Wiley and Sons: New York, 1970.
(27) Siebert, H. *Z. Anorg. Allg. Chem.* **1954**, *275*, 225.
(28) Billes, F.; Mikosch, H.; Holly, S. *J. Mol. Struct.* **1998**, *423*, 225.

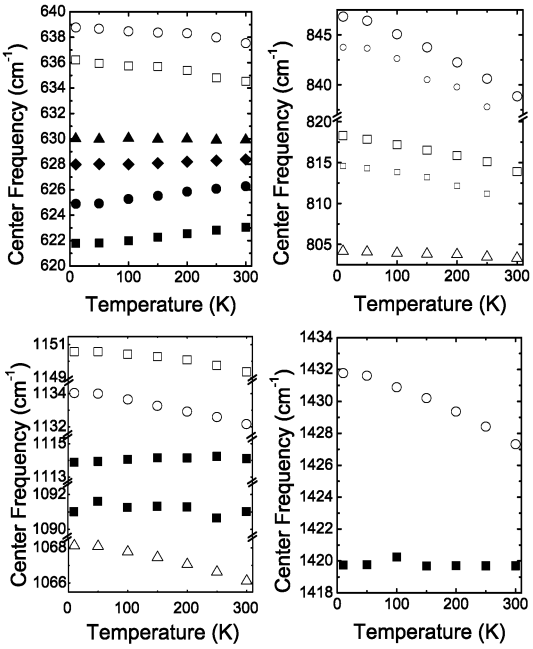

Figure 4. Temperature dependence of center frequencies of the modes shown in Figure 3. The smaller symbols in the upper right-hand panel refer to satellite modes associated with the main mode that is nearby and denoted by the larger symbol. The error bar is on the order of the symbol size.

ature (Figure 4). Here, the center frequencies of the softened or fixed-frequency modes are shown as solid symbols, to visually distinguish them from the more numerous modes that harden at low temperature. The 622 and 625 cm^{-1} modes red shift by ~0.7 and 1.4 cm^{-1} between 300 and 10 K, respectively. The magnitude of the red-shift is significantly less than that observed in the analogous 1D compound, $Cu(Pz)(NO_3)_2$.[19] Nevertheless, low-temperature mode softening is definitely observed in the $S = {}^1/_2$ square antiferromagnet. We attribute the low-temperature mode softening in $Cu(Pz)_2(ClO_4)_2$ to a change in hydrogen bonding interactions between the oxygens in the ClO_4^- counterion and the pyrazine ring hydrogens. Considering the electronegativity of oxygen, it is reasonable for the ClO_4^- counterions to be involved in hydrogen bonding in this system. From this point of view, the fixed-temperature modes near 1090 and 1115 cm^{-1} may be components of the $\nu_3(ClO_4)$ mode. The other temperature-independent mode at 1420 cm^{-1} may be indicative of a weak hydrogen bonding interaction involving the hydrogen atoms of the pyrazine rings. Thus, the assignments and behavior of the fixed-frequency modes (Figures 3 and 4) support our supposition of a hydrogen bonding interaction between the oxygens of ClO_4^- and the hydrogens of the pyrazine rings in $Cu(Pz)_2(ClO_4)_2$, similar to that observed in the 1D analogue $Cu(Pz)(NO_3)_2$.

Extensive low-temperature mode softening in the 1D $Cu(Pz)(NO_3)_2$ was recently observed by Jones et al.[19] The mode softening was interpreted in terms of enhanced electrostatic attraction between pyrazine hydrogens and nitrate oxygens as the lattice contracts at low temperatures. As the lattice contracts, the distance between oxygens and hydrogens becomes closer, rendering the attractive interaction stronger. Such a competing interaction against the thermal contraction consequently gives rise to the increase of certain bond lengths at low temperature and, thus, results in the softening of selected vibrational modes. This analysis was supported by X-ray diffraction data which show some bond lengths of $Cu(Pz)(NO_3)_2$ increase with decreasing temperature.[19]

In retrospect, it is not so surprising to find the mechanism of intermolecular hydrogen bonding, manifested by the low-temperature mode softening, important in both $Cu(Pz)(NO_3)_2$ and $Cu(Pz)_2(ClO_4)_2$. However, it is curious that only a few modes in the title compound soften (Figures 3 and 4), whereas nearly one-third of the modes soften at low temperature in $Cu(Pz)(NO_3)_2$. This difference may be attributed to the weaker interplanar interactions between the sheets in the 2D material compared to the interactions between the chains in the 1D sample. These weak contacts may also be viewed as acid−base interactions. In both materials, the bases, coordinated nitrate (NO_3^{2-}) ions for the 1D sample and perchlorate (ClO_4^-) ions in the 2D sample, interact with aromatic protons on nearby pyrazine rings. However, since the nitrate oxygen atoms are more basic than the oxygen atoms on the perchlorate ions, the hydrogen bonds and hence the interchain interactions in the 1D material are expected to be stronger than the intersheet interactions in the 2D sample. Another difference may be the structural "stiffness" of the 2D material compared to the 1D sample. The increased dimensionality of the 2D material may render interplanar movements more difficult than interchain motion in the 1D sample. In conjunction with the stronger acid−base interactions present, the number of red-shifted peaks as well as the magnitude of the red shift in the infrared spectrum associated with these weak interactions are expected to be greater for $Cu(Pz)(NO_3)_2$ (1D) than $Cu(Pz)_2(ClO_4)_2$ (2D).

In addition to the unusual frequency shifts that we associate with a change in hydrogen bonding in $Cu(Pz)_2(ClO_4)_2$, several infrared-active modes display clear evidence of low-temperature symmetry breaking. These include the following: the cluster near 500 cm^{-1}, the features near 800 cm^{-1}, and the modes near 1420 cm^{-1}, all of which are assigned to pyrazine ring motion (Table 1). Using the 300 K doublet near 500 cm^{-1} as an example, this structure splits into quadruplets with decreasing temperature, with small satellite peaks ~7 cm^{-1} above the two main features. We attribute the aforementioned fine structure to two different low-temperature pyrazine sites. As in other materials, the lowest energy peak in the doublet is more intense.[29] We quantify these effects in Figure 5 by plotting the normalized integrated oscillator strength of both the 498 and 510 cm^{-1} satellite peaks as a function of temperature. The oscillator strength of both modes increases gradually with decreasing temperature, saturating near 150 K. Taking the integrated oscillator strength of these satellite bands as the square of the order parameter,[29−33]

(29) Musfeldt, J. L.; Kamarás, K.; Tanner, D. B. *Phys. Rev. B* **1992**, *45*, 10197.
(30) Bozio, R.; Pecile, C. *Solid State Commun.* **1981**, *37*, 193.
(31) Bozio, R.; Pecile, C. *J. Phys. C: Solid State Phys.* **1980**, *13*, 6205.
(32) Rice, M. J. *Phys. Rev. Lett.* **1976**, *37*, 36.
(33) In this Figure 6, the oscillator strengths have been normalized with respect to the limiting low-temperature value of the intensity of each mode.

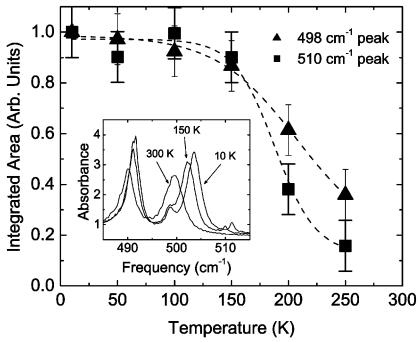

Figure 5. Normalized oscillator strength of two sideband modes associated with pyrazine ring out-of-plane deformation vs temperature. The inset shows a close-up view of these spectral features.

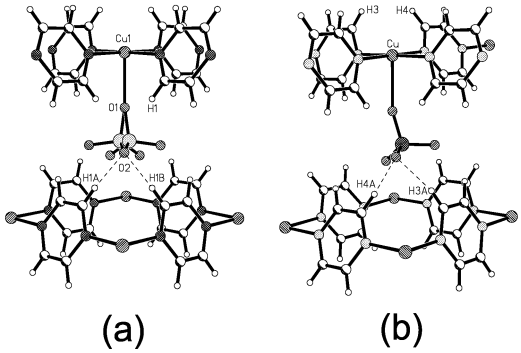

Figure 6. Packing structure of $Cu(Pz)_2(ClO_4)_2$ at room temperature (a) and 163 K (b), illustrating the proposed hydrogen bonding. Symmetry transforms: A ($-x$, $1 - y$, $-z$); B ($-x$, y, $-z$) at room temperature (a) and A ($x - 0.5$, $-y - 0.5$, $z + 0.5$) at 163 K (b).

we suggest that $Cu(Pz)_2(ClO_4)_2$ has a second-order structural phase transition near ~180 K.[34] As discussed in following paragraphs, the transition seems to be of order−disorder type.

Single crystal X-ray analysis of $Cu(Pz)_2(ClO_4)_2$ supports the aforementioned correlation between the vibrational response and intermolecular hydrogen bonding.[35] These results are summarized in Table 2. At 293 K, the material crystallizes in the monoclinic space group *C*2/*m*, whereas at 163 K, the space group is *C*2/*c*, evidence for a subtle structural phase transition. The perchlorate ions are disordered across the mirror plane at room temperature, but order at low temperature, with a concomitant doubling of the unit cell. In addition to the change in the structure of the perchlorate ions, there is a change in the behavior of the pyrazine rings. At 293 K, the pyrazine moieties are equivalent by symmetry, giving a square layer, whereas at 163 K, the two inequivalent pyrazine molecules result in a herringbone pattern within the layer.

Table 2. Crystal Data and Structure Refinement for $Cu(Pz)_2(ClO_4)_2$

	room temp	low temp
empirical formula	$C_8H_8N_4O_8Cl_2Cu$	$C_8H_8N_4O_8Cl_2Cu$
fw	422.62	422.62
cryst syst	monoclinic	monoclinic
cryst habit	cubic prism	irr block
space group	*C*2/*m*	*C*2/*c*
	Unit Cell Dimensions	
a (Å)	9.734(2)	14.072(5)
b (Å)	9.729(2)	9.786(3)
c (Å)	8.1320(17)	9.781(3)
α (deg)	90	90
β (deg)	120.855(4)	96.458(4)
γ (deg)	90	90
V (Å^3)	661.1(2)	1338.3(7)
Z	2	4
D (calcd) (g/cm^3)	2.123	2.098
size (mm^3)	0.08 × 0.08 × 0.08	0.13 × 0.44 × 0.76
F(000)	422	844
μ (mm^{-1})	2.109	2.084
	Data Collection:	
temp (K)	293(2)	163(2)
reflns collected	2985	7980
indep reflns	991 [R_{int} = 0.0255]	1417 [R_{int}=0.0546]
θ range (deg)	2.92−30.63	2.54−27.08
range *h*,*k*,*l*	$-13 \le h \le 13$	$-17 \le h \le 17$
	$-13 \le k \le 11$	$-12 \le k \le 12$
	$-11 \le l \le 11$	$-7 \le l \le 12$
	Refinement	
data/restraints/params	991/0/77	1417/0/117
GOF on F^2	1.056	1.107
final *R* indices [$I > 2\sigma(I)$]		
R1	0.0311	0.0600
wR2	0.0791	0.1543
R indices (all data)		
R1	0.0331	0.0614
wR_2	0.0801	0.1556
largest diff peak (e/Å^3)	0.483	2.508 (near N1)
largest diff hole (e/Å^3)	−0.231	−1.312 (near Cu)

Figure 6 shows a close-up view of the counterion pocket in $Cu(Pz)_2(ClO_4)_2$. The order−disorder transition results in a change in hydrogen bonding between the perchlorate ion and the hydrogens of the pyrazine ring. At room temperature, there are two equivalent hydrogen bonds between O2 (not disordered) and the two symmetry-equivalent H1 atoms: $d_{O2\cdots C1} = 3.09$ Å, $d_{C1-H1} = 0.88$ Å, $d_{H1\cdots O2} = 2.49$ Å, and $\angle_{C1-H1\cdots O2} = 126°$. At low temperature, the structural phase transition results in two inequivalent hydrogen bonds to O2: one each to H3A and H4A. In this case, $d_{O2\cdots C4A} = 3.05$ Å, $d_{C4A-H4A} = 0.93$ Å, $d_{H4A\cdots O2} = 2.44$ Å, $\angle_{C4A-H4A\cdots O2} = 123°$; $d_{O2\cdots C3A} = 3.18$ Å, $d_{C3A-H3A} = 0.90$ Å, $d_{H4A\cdots O2} = 2.65$ Å, and $\angle_{C4A-H4A\cdots O2} = 119°$. While the hydrogen bonding modifications that result from the phase transition/symmetry change are subtle, they are clear and provide structural support for the observed changes in the infrared spectra, reported here.

IV. Conclusion

We report the variable-temperature vibrational response of $Cu(Pz)_2(ClO_4)_2$. With decreasing temperature, the majority of modes harden as expected; however, a few ClO_4^- related modes display unusual softening. Several other modes, related to the motion of the pyrazine ring, are temperature independent. We attribute this low-temperature behavior to an enhanced hydrogen bonding interaction between the oxygens of the ClO_4^- anions and the hydrogens of the pyrazine

(34) As with any second-order transition, the physical properties change over a range of temperatures, without a sharp discontinuity in the order parameter. For $Cu(Pz)_2(ClO_4)_2$, we find $T_c \sim 180$. This choice is based upon the decay of the integrated oscillator strength of the sidebands with temperature, as shown in Figure 5. The sidebands decay most rapidly near 180 K, with clear evidence for fluctuation effects above the transition temperature.

(35) Crystallographic data for the structure of $Cu(Pz)_2(ClO_4)_2$ have been deposited with the Cambridge Crystallographic Data Centre as supplementary publication no. CCDC-203408 (293 K) and CCDC-203407 (163 K). Copies of the data can be obtained from CCDC, 12 Union Road, Cambridge CB2 1EZ, U.K. [Fax: int code + 44(1223)-336-033. E-mail: deposit@ccdc.cam.ac.uk].

rings, similar to that observed in the 1D analogue $Cu(Pz)(NO_3)_2$. However the degree of mode softening in $Cu(Pz)_2(ClO_4)_2$ is much less than that in $Cu(Pz)(NO_3)_2$, suggesting that the hydrogen bonding interactions in the title compound are weaker than in $Cu(Pz)(NO_3)_2$, and the structure is more robust due to the square planar nature of the lattice. We also explored the connection between the subtle second-order order−disorder transition and the vibrational properties. The main consequence of the low-temperature ClO_4^- ordering and two pyrazine positions is the aforementioned change in hydrogen bonding and the splitting of Pz-related vibrational modes. We speculate that low-temperature hydrogen bonding enhancement may be a common feature of copper−pyrazine-based materials.

Acknowledgment. This project was supported by the Materials Science Division, Basic Energy Sciences at the U.S. Department of Energy (DE-FG02-01ER45885) and the Division of Material Research at the National Science Foundation (DMR-9803813) at the University of Tennessee and Clark University, respectively.

CM030049E